Comparison of the performances of different spring and superconducting gravimeters and STS-2 seismometer at the Gravimetric Observatory of Strasbourg, France

SEVERINE ROSAT[1], MARTA CALVO[1,2], JACQUES HINDERER[1], UMBERTO RICCARDI[3], JOSE ARNOSO[4] AND WALTER ZÜRN[5]

1 Institut de Physique du Globe de Strasbourg, UMR 7516, Université de Strasbourg/EOST, CNRS, 5 rue Descartes, 67084 Strasbourg Cedex, France (Severine.Rosat@unistra.fr)

2 Observatorio Geofísico Central, Instituto Geográfico Nacional (IGN), Madrid, Spain

3 Dipartimento di Scienze della Terra, dell'Ambiente e delle Risorse (DiSTAR), Università Federico II di Napoli, Naples, Italy

4 Instituto de Geociencias (CSIC, UCM), Madrid, Spain

5 Black Forest Observatory of Karlsruhe Institute of Technology and University of Stuttgart, Heubach 206, D-77709 Wolfach, Germany

Received: May 15, 2014; Revised: August 2, 2014; Accepted: August 7, 2014

ABSTRACT

Since 1973, the Gravimetric Observatory of Strasbourg (France) is located in an old fort named J9 and has been the place for various gravity experiments. We present a comparison of the noise levels of various instruments that are or were continuously recording at J9, including the LaCoste&Romberg Earth-Tide Meter ET-5 (1973–1985), the GWR Superconducting Gravimeter TT-T005 (1987–1996), the Superconducting Gravimeter C026 (since 1996), the STS-2 seismometer (since 2010) and the LaCoste&Romberg ET-11 (continuously since October 2010). Besides these instruments, the J9 Observatory has hosted temporary gravity experiments with the Micro-g LaCoste Inc. gPhone-054 (May–December 2008 and May–September 2009) and the Micro-g LaCoste Inc. Graviton-EG1194 (June–October 2011). We include also in the comparison the absolute gravimeter Micro-g FG5 #206 which is regularly performing absolute gravity measurements at J9 since 1997 and a spring gravimeter Scintrex CG5 which recorded at J9 between March 2009 and February 2010. We present the performances of these various instruments in terms of noise levels using a standardized procedure based on the computation of the residual power spectral densities over a quiet time period. The different responses to atmospheric pressure changes of all the instruments are also investigated. A final part is devoted to the instrumental self-noise of the SG C026, STS-2 and L&R ET-11 using the three channel correlation analysis method applied to 1-Hz data.

Stud. Geophys. Geod., 59 (2015), 58–82, DOI: 10.1007/s11200-014-0830-5

Keywords: superconducting gravimeter; spring gravimeter; broad-band seismometer; power spectral density; noise level; barometric admittance; three-channel correlation

1. INTRODUCTION

At the beginning of the 70s, the gravimetric observatory of Strasbourg was installed in an old bunker named J9 located about 10 km north of Strasbourg in the top of a sedimentary hill. Since then, gravity variations have been observed and recorded with spring, superconducting and absolute gravimeters. The first observations at J9 were performed with an Askania gravimeter belonging to M. Bonatz, which was recording for 77 days spanning the end of 1971 and beginning of 1972. After that, a Geodynamics gravimeter was installed by P. Melchior and J.T. Kuo in 1973. Later on a LaCoste & Romberg ET005 improved by R. Lecolazet and J. Gostoli in 1970 with an electrostatic feedback system and a digital acquisition, was recording with a sampling interval of 1 h (*Gostoli, 1970*; *Abours, 1977*; *Abours and Lecolazet, 1977*). Here we will focus on the period starting in 1976 with the latest improved version of the L&R ET005 that was recording time-varying gravity till mid-1985. Then in 1987, a new era of gravimetry began with the installation of a first GWR superconducting gravimeter TT070-T005, followed without any interruption by the installation in 1996 of a more compact one, the C026. The SG C026 has been recording continuously since then. Since October 2010, a broad-band seismometer STS-2 and a modified LaCoste & Romberg ET-11 (using electrostatic feedback) are recording side by side on a Quanterra (Q4120) data logger system. Besides these permanent installations, the J9 observatory has temporarily hosted several spring gravimeters: a Scintrex CG5 (March 2009 – February 2010), the Micro-g LaCoste Inc. gPhone-054 with the PET (Portable Earth Tide gravimeter) system (May–December 2008 and May–September 2009) owned by the Instituto Geografico Nacional (IGN) of Madrid in Spain and the LaCoste & Romberg Graviton-EG1194 (hereafter referred as Graviton) owned by the Instituto de Geociencias of Madrid (June – October 2011). Finally, regular absolute gravity measurements with the Micro-g FG5 #206 have been performed at J9 since 1997. A summary of the instruments recording at J9 since 1976 is plotted in Fig. 1 and Table 1 gives their respective sampling rates, built-in filters (if any), scale factors and digital acquisition systems. We refer to *Crossley et al. (2013)* for a summary of the general specifications of absolute and relative gravimeters and to *Richter et al. (1995)* for an interesting comparison of an SG, L&R ET-19 and STS-2 and STS-1 seismometers at Black Forest Observatory (Germany). The respective transfer functions of these instruments are also plotted in the latter paper.

In a first part we will present the performances of these various instruments in terms of noise levels using a standardized procedure based on the computation of the residual power spectral densities over a quiet time period in the seismic (periods smaller than 1 h) and in the sub-seismic (between 1 h and 6 h) frequency bands. As we do not have long enough records for all the instruments, the comparison at tidal frequencies is not shown here. We can refer to *Riccardi et al. (2011)* for some past comparison of the gPhone-054, Scintrex CG5 and SG C026 at tidal frequencies, to *Hinderer et al. (2002)* for a previous comparison between the SG C026, STS-2 and FG5#206, to *Arnoso et al. (2014)* for

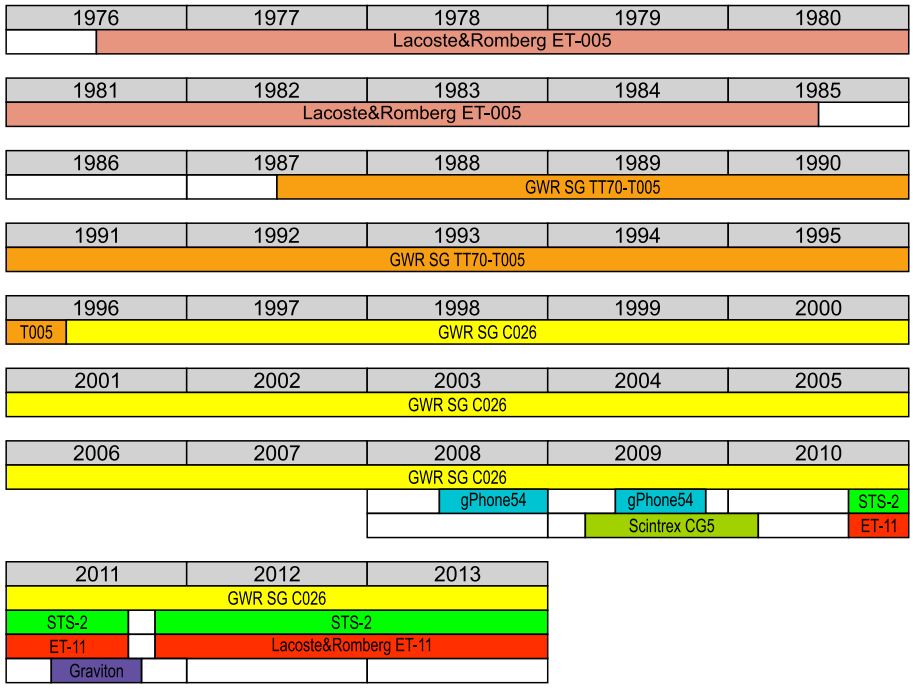

Fig. 1. Operation time of the relative gravimeters and seismometer recording at J9 since 1976 till now.

a comparison between the SG C026 and Graviton and to *Calvo et al. (2014)* for a comparison of the tidal analysis results between the two SGs and the L&R ET005. In a second part, the response of the relative instruments to atmospheric pressure and to ambient temperature changes is investigated. Finally, we will use a three-channel correlation analysis to measure the instrumental noise of digitizers and seismic/gravimetric sensors following a technique proposed by *Sleeman et al. (2006)* applied to the de-tided SG C026, L&R ET11 and STS-2 data.

2. NOISE LEVEL COMPARISON

The common way to estimate the noise level at an instrumental site is to compute power spectral densities (*PSD*s). A standard procedure was developed by *Banka (1997)* and *Banka and Crossley (1999)* to compute the noise level (instrumental plus environmental) at seismic frequencies. Later on, *Rosat et al. (2004)* generalized this procedure to compute the noise levels of SG sites belonging to the GGP (Global Geodynamics Project) network (*Crossley et al., 1999*) at longer periods (sub-seismic and tidal frequencies). An updated comparison of the SG seismic noise was published by *Rosat and Hinderer (2011)* who have shown that the noise at the GGP sites was quite stable in time.

Table 1. List of the gravimeters and seismometer used in this study with their respective sampling rates, built-in filters, scale factors, sensitivities and analysis periods.

Sensor	Sampling Rate [s]	Built-in Filter	Resolution [nm/s^2]	Scale Factor [nm/s^2/V]	Analysis Period for Barometric Admittance	A/D Converter
SG T005	300	TIDE-filter: low-pass filter, corner period around 100 s	0.1	–760.2		Home-made
SG C026		yes	0.1	–792.0		
raw	1	2-pole Bessel filter; corner frequency: 5 s				Home-made
GGP-1	1	8-pole Bessel filter; corner frequency: 16 s			2012/01/05-2012/01/20	GWR
GGP-2	2	8-pole Bessel filter; corner frequency: 32 s				Home-made (till 2009), then GWR
LaCoste & Romberg ET005	3600	yes	10		1978/11/29-1978/12/14	Home-made
LaCoste & Romberg ET-11	1	yes	10	916	2012/01/05-2012/01/20	Quanterra Q4120
Scintrex CG5	60	no (initial sampling at 6 Hz then averaging to 1 min)	10	Output in gravity units	2009/11/06-2009/11/20	Own
Micro-g LaCoste gPhone-054	60	no	10	–5206*	2009/06/01-2009/06/15	Own
Micro-g LaCoste Graviton-EG1194	60	Initial sampling > 1 Hz then 30 s FIR low-pass filter before decimation	10	Output in gravity units	2011/08/09-2011/08/23	Own
STS-2	1	Initial sampling 32 kHz then analog signal enhancement, digital signal processing and decimation → basic output sampling frequency 1 kHz, then FIR filters to 1 Hz	Transfer function with 2 poles and 2 zeroes Sensitivity of 6.01559 10^8 V/m/s at 0.02 Hz		2012/01/01-2012/01/16	Quanterra Q4120

* *Riccardi et al. (2011)*

Here we will apply the procedure summarized in *Rosat et al. (2004)* for seismic and sub-seismic frequencies. As the instruments are located in the same environment of the J9 bunker, the environment of which has not been modified in terms of anthropogenic noise over the 4 decades considered here, and supposing that the different pillars have similar effects on the records, the differences of noise levels can be interpreted as being purely instrumental (sensor plus data acquisition system). Indeed, from these specific data sets one cannot make general statements about all the instruments of a type. We only provide an example of their performances in this paper.

We consider raw calibrated gravity records. The relative superconducting gravimeters were calibrated using repetitive co-located absolute gravity measurements, while the spring gravimeters were calibrated using a local tidal model (inferred from SG C026 data analysis) for the L&R ET-11 and a purely theoretical body tide model for the L&R ET-005. For the gPhone, Graviton and CG5, the calibration used was given by the manufacturer. For the STS-2, we have employed the nominal transfer function. We have computed residual data by removing a local tidal model and the local atmospheric pressure effect using a nominal admittance of -3 (nm/s^2)/hPa. The atmospheric pressure changes have been continuously recorded by high quality barometers (Schlumberger, Druck DPI and Paroscientific models) in parallel with the continuous gravity measurements since 1973. We will see in Section 3 that removing the atmospheric pressure effects through the classical admittance approach is inefficient for some of the spring meters and for the STS-2 because of the poor coherency with atmospheric pressure changes.

At seismic frequencies, we consider 5 quiet days and remove a 9th-degree polynomial drift. At sub-seismic frequencies, we consider the quietest period of 15 continuous days and we remove a linear drift before applying a high-pass filtering with a cut-off period of 8 h. The *PSD* is then estimated using a smoothed periodogram.

First the procedure is applied at seismic frequencies to the L&R ET005, L&R ET-11, SG T005, SG C026, gPhone-054, Scintrex CG5, Graviton and the STS-2. The L&R ET005 had a sampling rate of 1 h, the SG T005 of 5 min, the Scintrex CG5 (the 1-min output is indeed a simple average of raw 6-Hz samples) and Graviton of 1 min (the raw data is low-pass filtered with a finite-impulse-response - FIR - filter of length 30 s before recording the 1-min samples), while the SG C026, gPhone-054 and L&R ET-11 are sampled at 1 s. The data from the latter three sensors were down-sampled to 1-min interval after low-pass filtering. Note also that in the procedure, a 9th-degree polynomial fit is removed for each instrument so that the *PSD*s are artificially flat at periods longer than 6 h, except the FG5 for which no polynomial fit has been removed because of the short available data length. In Fig. 2 we show the *PSD*s for the whole dataset with sampling intervals of 1-minute or longer together with the Low Noise Model (NLNM) of *Peterson (1993)*. The data were not corrected for instrument or filter responses.

For the absolute gravimeter FG5, we only have segments of a few continuous days available during the calibration experiments for the SG at an hourly sampling (set values). It is well-known that the *PSD*s of absolute measurements are aliased by the microseismic noise (see e.g. *Crossley et al., 2001*). A higher rate of drops (every drop corresponds to the free fall of the object) which is presently performed every 10 s is necessary to avoid this aliasing. We have obtained a noise level at 10^{-4} Hz around -125 dB (Fig. 2) which is

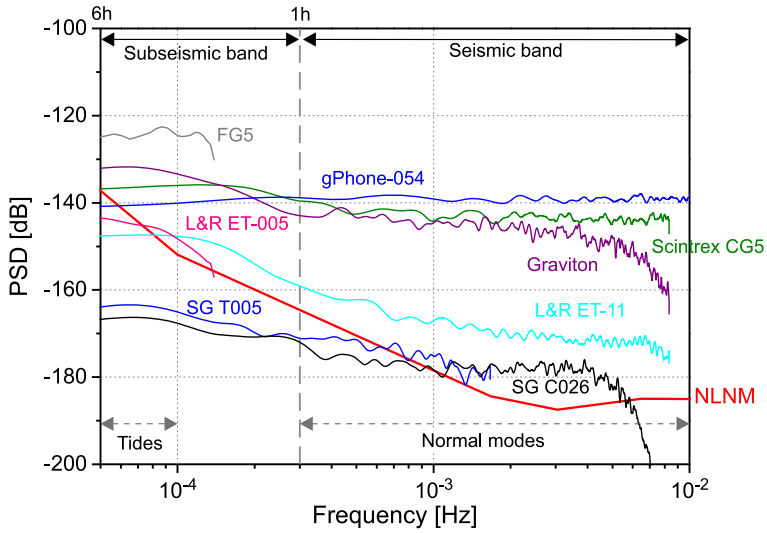

Fig. 2. Power Spectral Densities (*PSD*) relative to 1 $(m/s^2)^2$/Hz during the 5 most quiet days of spring and superconducting gravimeters with a sampling period of 1 min or larger. The *PSD* for the absolute gravimeter FG5 is also plotted. The NLNM (New Low Noise Model) of *Peterson (1993)* is shown for reference. The data were not corrected for instrument or filter responses.

in agreement with the results by *Crossley et al. (2001)* and *Hinderer et al. (2002)*. Using AG drops sampled at higher frequency, *Van Camp et al. (2005)* obtained slightly lower *PSD* levels. The noise level of their FG5#202 at station Membach (Belgium) ranges between −130 dB and −140 dB when the microseismic noise is high and low, respectively, and is flat at periods shorter than one day (under white noise assumption).

From Fig. 2 we can say that the *PSD*s roughly fall into three groups: SGs with the lowest *PSD* levels, ETs in the middle and other spring gravimeters with the highest *PSD* levels. It appears that the older ET gravimeters perform appreciably better than the more modern spring instruments in the long-period seismic frequency band. Indeed the ET feedback system includes a low-pass filter with a 1-min cutoff while for the CG5 the output 1-min data are obtained by simply averaging the raw 6-Hz data. Between the SG T005 and SG C026, we can see an improvement in the noise level which is due to an upgrade of the instrument and of the acquisition system.

In Fig. 3 we show the *PSD*s computed on the 5 quietest days for the instruments for which we had a 1-Hz sampling besides the 1-min sampled Graviton and Scintrex CG5.

The *PSD* of the ET-11 drops off at high-frequencies because of the instrumental feedback. The SG C026 electronics (GEP-2) has several outputs with different electronic filters: raw gravity (the signal comes directly from the current through the feedback coil for the sphere after low-pass filtering with a simple two-pole filter having a 0.2 Hz corner frequency) and GGP1 (or GGP2 before May 2010) low-pass filtered gravity using an eight-pole Bessel filter with corner frequencies 30.8 mHz (GGP2) or 61.5 mHz (GGP1) which makes the *PSD* drop off at higher frequencies. The scale factors of the SG C026

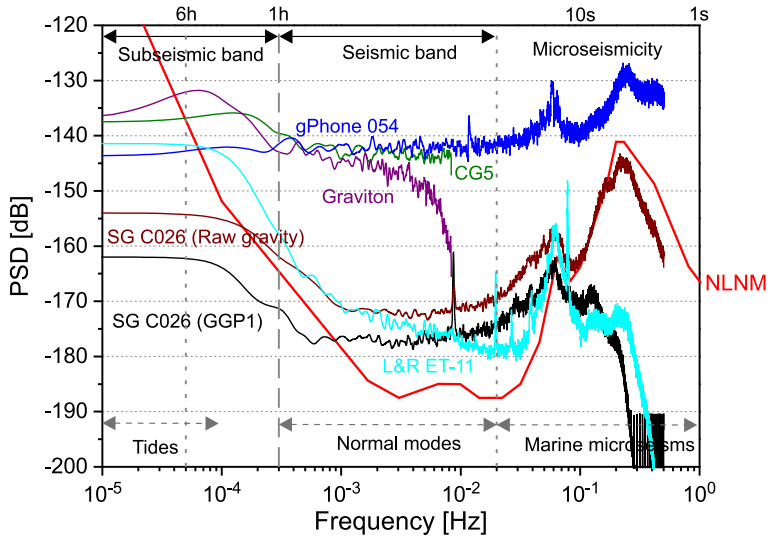

Fig. 3. Power Spectral Densities (*PSD*) relative to 1 $(m/s^2)^2$/Hz during the 5 most quiet days of spring and superconducting gravimeters with a sampling rate of 1 Hz (gPh54, L&R ET-11, SG C026) and sampling interval 1 min (CG5 and Graviton). The NLNM (New Low Noise Model) of *Peterson (1993)* is shown for reference.

(GGP2 and then GGP1 channels) and SG T005 were estimated by co-located absolute measurements (see e.g. *Amalvict et al., 2001*; *Rosat et al., 2009*; *Calvo et al., 2014*). For the raw gravity channel of the SG C026, we have checked the calibration by comparing with a local tidal model. Please note that this raw gravity output was digitized at 1 Hz using a home-made acquisition unit, independent of the GWR digital acquisition unit. This home-made acquisition unit was tested against the GWR DAU to check that it does not introduce any additional noise. As the gPhone-054 data are not filtered, we also plot the *PSD* of the 5 quietest days for the raw gravity output of the SG C026 in Fig. 3 for a fair comparison with the gPhone-054. As already noted by *Riccardi et al. (2011)*, the gPhone-054 and the CG5 are roughly 20 dB noisier than the SG C026 at seismic frequencies. The *PSD* level of the raw gravity output channel of the SG C026 is larger than the *PSD* of the GGP2 gravity output because of the aliasing of some high-frequency noise. This noise could, for instance, be caused by vibrations excited by the refrigeration system (*Imanishi, 2009*) or by the sequence of peaks appearing above 0.25 Hz in Fig. 3 in the *PSD* of the GGP-1 filter. These peaks are of nearly equal amplitude (at a level below -190 dB after filtering), are regularly spaced every 1/60 Hz, and always present in the data. In our opinion they are caused by regular spikes every minute in the time series which originate from a mechanical switch used to scan between the auxiliary data channels for the SG C026 GWR DAU. A similar spectral behavior with equispaced spikes was indeed found on the amplitude spectrum of the FG5 superspring signal (not gravity) and attributed to mechanical disturbances (floor recoil) appearing at every drop during each set (sequence of consecutive drops of the prism) (*Hinderer et al., 2002*). Such spikes are

not present at newer SG sites since more recent GWR DAUs record the auxiliary channels at 1 Hz without a mechanical switch. The 5 quietest days (used for Fig. 3) differ for each instrument because of instrumental disturbances and differences in the response to ambient pressure and temperature as we will see in the next part. As a consequence, the amplitude of the microseismic noise is different for each *PSD* plot. Therefore we have also plotted in Fig. 4 the *PSD*s computed on the same 5 quiet days for the 1-Hz data of the (a) L&R ET-11, SG C026 and STS-2 (days 178, 212, 213 and 226 of year 2012 and day 214 of year 2011) and (b) SG C026 (raw gravity and GGP2 filter) and gPhone-054 (day 235 of year 2008, days 181, 183, 185 and 186 of year 2009). We can see the marine microseismic peak very clearly in the data from the raw SG C026 and the gPhone-054. A similar high ocean noise at about −130 dB (equivalent to a signal to noise amplitude SNA of 300 $nm/s^2/Hz^{1/2}$) was also observed in the noise level of a PET gravity meter installed far from the oceans, in Boulder (Colorado), by *Niebauer (2007)*. He obtained a *PSD* level around −154 dB (*SNA* = 20 $nm/s^2/Hz^{1/2}$) in the normal mode band while our PET gPhone-054 has a higher noise level (around −140 dB).

At the period of 2 min, we can see the parasitic resonance of the sphere of the SG. We see in the *PSD* of the L&R ET-11 some oscillations at 50 s, 25 s and 12.5 s. They are due to the heating cycles of the gravimeter having two nested thermostats, one in the inner shield and one in the outer shield. Indeed, the heater cycles were manually measured twice in July 2013 and April 2014. The measurements revealed that the inner heater cycle was between 13.9 s and 14 s in April 2014 with an on-part of 3.5 s and around 12 s in July 2013 with an on-part of 9 s. As for the outer heater cycle it was 38.5 s in total in July 2013 with an on-part of 32.5 s while in April 2014 it was larger than 30 min and could not be measured manually. Unluckily we did not measure the heater cycles in 2011 and 2012 but we can suppose that the 12.5 s spectral peak is due to the inner heater while the 50 s peak could be due to the outer heater. Using time-frequency spectrograms, we have checked the heater cycles, and it turned out that the outer heater has a very variable cycle in time and may be irregular during some time intervals, while the inner heater cycle is roughly constant between 12.5 s and 14 s. The on-time of the inner heater cycle being smaller than the on-time of the outer heater means that the outer heater brings the gravimeter to a temperature where the inner heater only needs to briefly heat the instrument while the outer heater cycle is adjusted to the ambient temperature.

Now we turn to the *PSD*s of the residuals on quiet 15-day periods for each instrument, except the Graviton as the data length available is not sufficient to retrieve a quiet period of 15 continuous days. The corresponding noise levels are plotted in Fig. 5. As in the seismic band, the *PSD*s of the gPhone and CG5 are much higher than for the SGs C026 and T005 (about 20 dB larger at a 3 h period). In the *PSD* of the SG C026 we can observe a peaky structure between 2 and 6 mHz corresponding to the continuous background oscillations, the so-called "hum" (e.g. *Nawa et al., 1998*; *Webb, 2007*; *Kurrle and Widmer-Schnidrig, 2008*; *Tanimoto, 2008*).

The performances of the LaCoste-Romberg ET-gravimeters are known to be quite competitive with SGs in some frequency bands (*Zürn et al., 1991*). Indeed, the L&R ET005 and ET-11 have lower noise levels than the CG5, Graviton or gPhone. However, although the performance of the L&R ET-11 was quite good in the seismic band, we see that at longer periods its noise level is very large, even higher than the L&R ET005. This

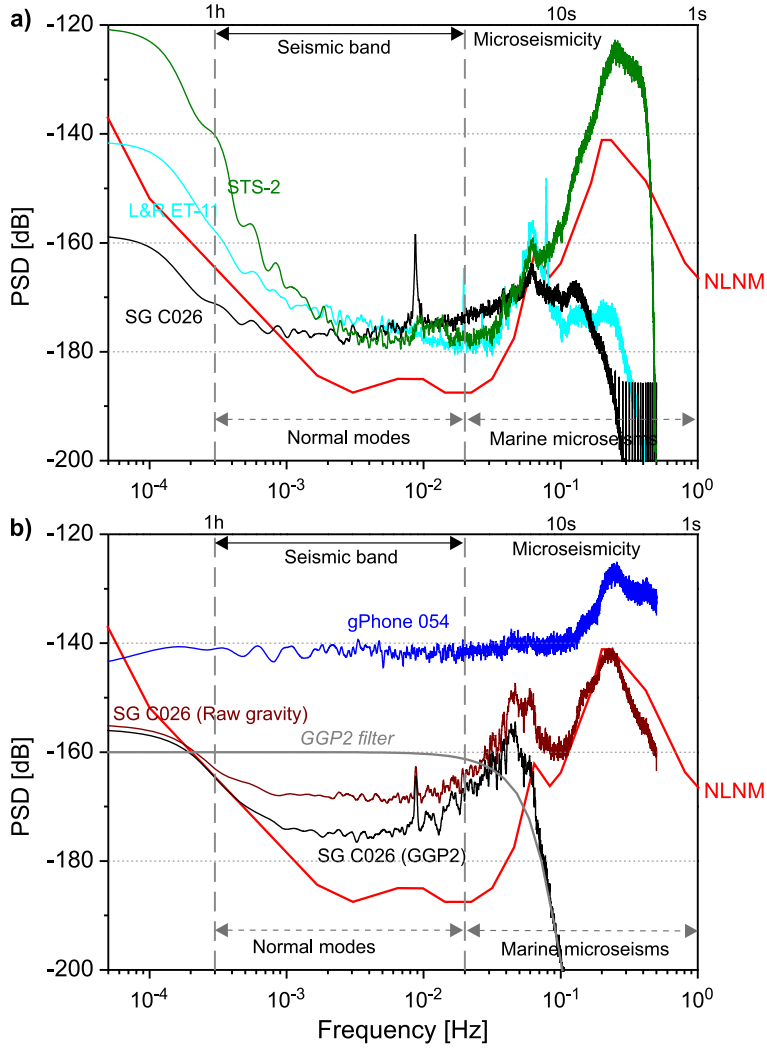

Fig. 4. Power Spectral Densities (*PSD*) relative to 1 $(m/s^2)^2$/Hz during the 5 most quiet days of **a)** L&R ET-11, SG C026 and STS-2 (days 178, 212, 213 and 226 of year 2012 and day 214 of year 2011); **b)** SG C026 (raw gravity and GGP2 filter) and gPhone-054, with a sampling rate of 1 Hz (day 235 of year 2008, days 181, 183, 185 and 186 of year 2009). The NLNM (New Low Noise Model) of *Peterson (1993)* is shown for reference.

is due to the fact L&R ET005 was operating inside a sealed metal container with constant inside pressure and thermostatically regulated (*Abours, 1977*) thus shielding the instrument against pressure and temperature changes and also the pressure seals of the currently operating L&R ET-11 have become leaky as we will confirm in the following section.

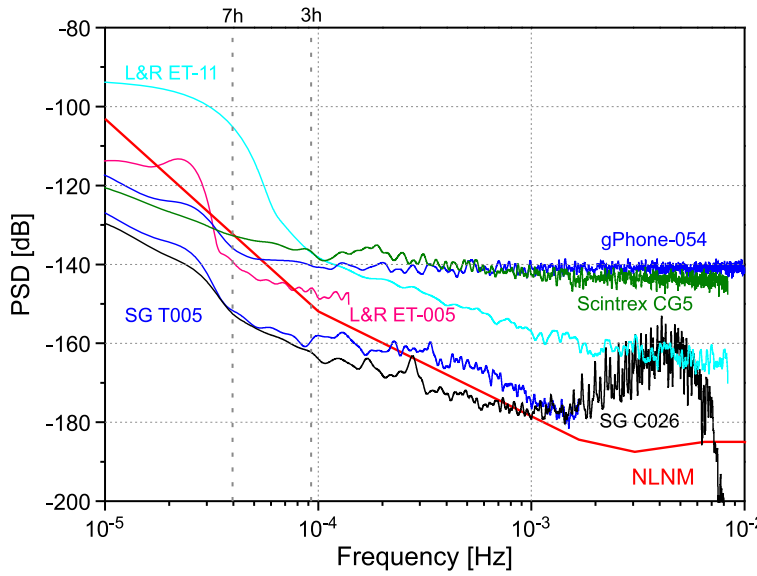

Fig. 5. Power Spectral Densities (*PSD*) relative to 1 $(m/s^2)^2$/Hz during the most quiet period of 15 days of L&R ET005, L&R ET-11, SG T005, SG C026, Scintrex CG5 and gPhone-054. The NLNM (New Low Noise Model) of *Peterson (1993)* is plotted for reference.

3. RESPONSE TO ATMOSPHERIC PRESSURE AND AMBIENT TEMPERATURE CHANGES

The response of the spring gravimeters and seismometers to air pressure variations often differs significantly from that of the SGs (e.g. *Freybourger et al., 1997*; *Riccardi et al., 2011*). In some cases, when the ET-instruments have good seals, they have the same response to barometric pressure as SGs (around −3.5 (nm/s^2)/hPa; *Widmer and Zürn, 1995*). The seals of the LaCoste & Romberg gravimeters become leaky after decades of operation and then Archimedean (buoyancy) effects act on the sensor mass in addition to the gravitation and loading by the atmosphere above the station. These effects are to a good part compensated by the internal buoyancy compensator (a large fixed volume of light mass) built into these instruments (mounted on the opposite side of the pivots as seen from the sensor mass, *LaCoste & Romberg, 2004*). If this were not the case, the effects of leaky seals would be much larger, as in seismometers and a change in atmospheric pressure would induce abnormal response of the instrument (e.g. *Arnoso et al., 2001*; *Meurers, 2002*). The gravitation and loading effects (about −3.5 (nm/s^2)/hPa) cannot be shielded and must therefore be seen by all the instruments.

At J9 each instrument is sensitive to the same outside pressure changes (true geophysical effect) which is similar to the ambient pressure as the rooms are not air locked.

Traditionally the atmospheric pressure effect is analyzed with frequency or time dependent admittances (e.g. *Merriam, 1992*; *Crossley et al., 1995*). In the following, we compute the coherency and the transfer function between the atmospheric pressure variations recorded at J9 and the gravity residuals (after drift and tides removal) of 1 min data over a period of 15 days for the L&R ET-11, gPhone, Graviton, CG5, STS-2 and 1 h data for the L&R ET005. In fact, on the graphs, we have plotted the squared coherence which is given by:

$$C_{xy} = \frac{\left|P_{xy}\right|^2}{P_{xx} P_{yy}},$$

where x is the pressure and y the gravity residuals. P_{xx} is the *PSD* estimate of x, P_{yy} is the *PSD* estimate of y and P_{xy} is the cross-*PSD* between x and y. The *PSD* is obtained using the Welch's averaged, modified periodogram method, i.e. the signals x and y are divided into eight sections with 50% overlap and tapered with a Hamming window. For each section a modified periodogram is computed and the eight periodograms are averaged.

The transfer function between gravity residuals and barometric data is computed by:

$$T_{xy}(f) = \frac{P_{yx}(f)}{P_{xx}(f)}.$$

The traditional frequency dependent admittance corresponds to the magnitude of this transfer function and the sign of the admittance is given by the cosine of the phase.

We have checked the L&R ET-005 response to atmospheric pressure changes. In Fig. 6a, we can see that the instrument drift after removal of solid Earth and ocean tides using a local tidal model is linear. After subtracting a linear drift, the obtained tidal residuals are clearly correlated to the atmospheric pressure changes and the coherence is 1 at low frequency and close to 0.8 at higher frequencies (cf. Fig. 6b). The drops of coherence are due to the presence of the S1 and S2 thermal tides in air pressure. The computed frequency-admittance over 15 days (between November 19 and December 14, 1978) is about –2.7 (nm/s^2)/hPa at long periods (i.e. periods larger than the 24 h thermal S1 tide) in agreement with the results of *Calvo et al. (2014)* and about –2 (nm/s^2)/hPa at frequencies larger than the S2 atmospheric tide. The tidal residuals are clearly improved after atmospheric pressure reduction as shown in Fig. 6b (lower plot). We conclude hence that the L&R ET005 was operating in normal conditions i.e. seals were good (maybe except for the phase shift of the effect, which is about 0° for tidal frequencies and ± 20° for frequencies larger than 10^{-5} Hz).

In the case of the L&R ET-11, the behavior is abnormal. Indeed, as shown in Fig. 7a, after removing a local tidal model, the tidal residuals are mostly correlated to the ambient temperature changes. After removing the temperature induced drift by least-squares fit to the ambient temperature measurements in the same room, the obtained residuals are only poorly correlated with the atmospheric pressure variations. This is clearly illustrated in Fig. 7b where the coherence with atmospheric pressure changes is weak at most frequencies. We have also tried to use the Hilbert-transform of the pressure variations as it

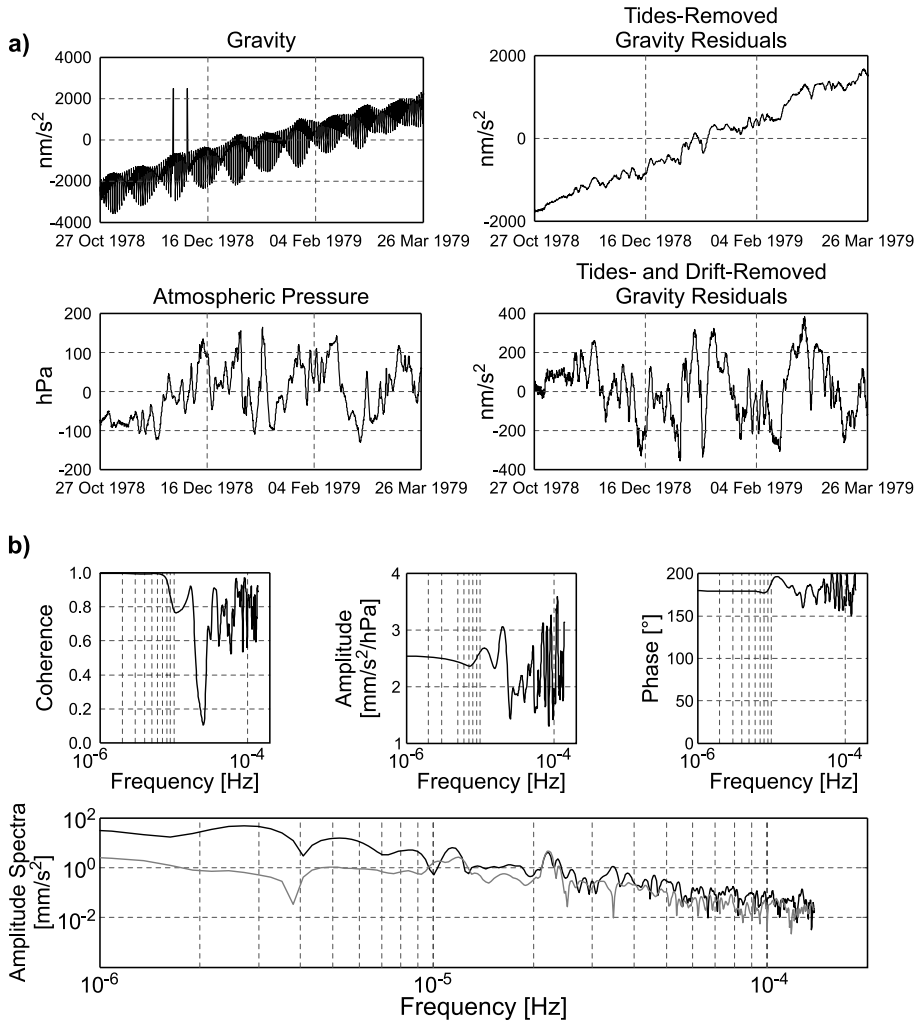

Fig. 6. L&R ET-005 response to atmospheric pressure changes: **a)** gravity records, tides-removed, tides- and drift-removed gravity residuals and atmospheric pressure variations; **b)** coherence, amplitude and phase response to pressure changes and amplitude spectra of tidal residuals before (in black) and after (in gray) atmospheric pressure reduction using the transfer function.

corresponds to a 90° phase shift of the pressure signal at all frequencies. Indeed the use of a single admittance with the Hilbert-transform of the pressure changes has proved to be efficient to correct horizontal accelerations (*Zürn et al., 2007*) as it corresponds to some physical model of acoustic waves travelling in the atmosphere. Leaky gravimeters still see the usual pressure effect but since the air density inside the instrument is modified, they

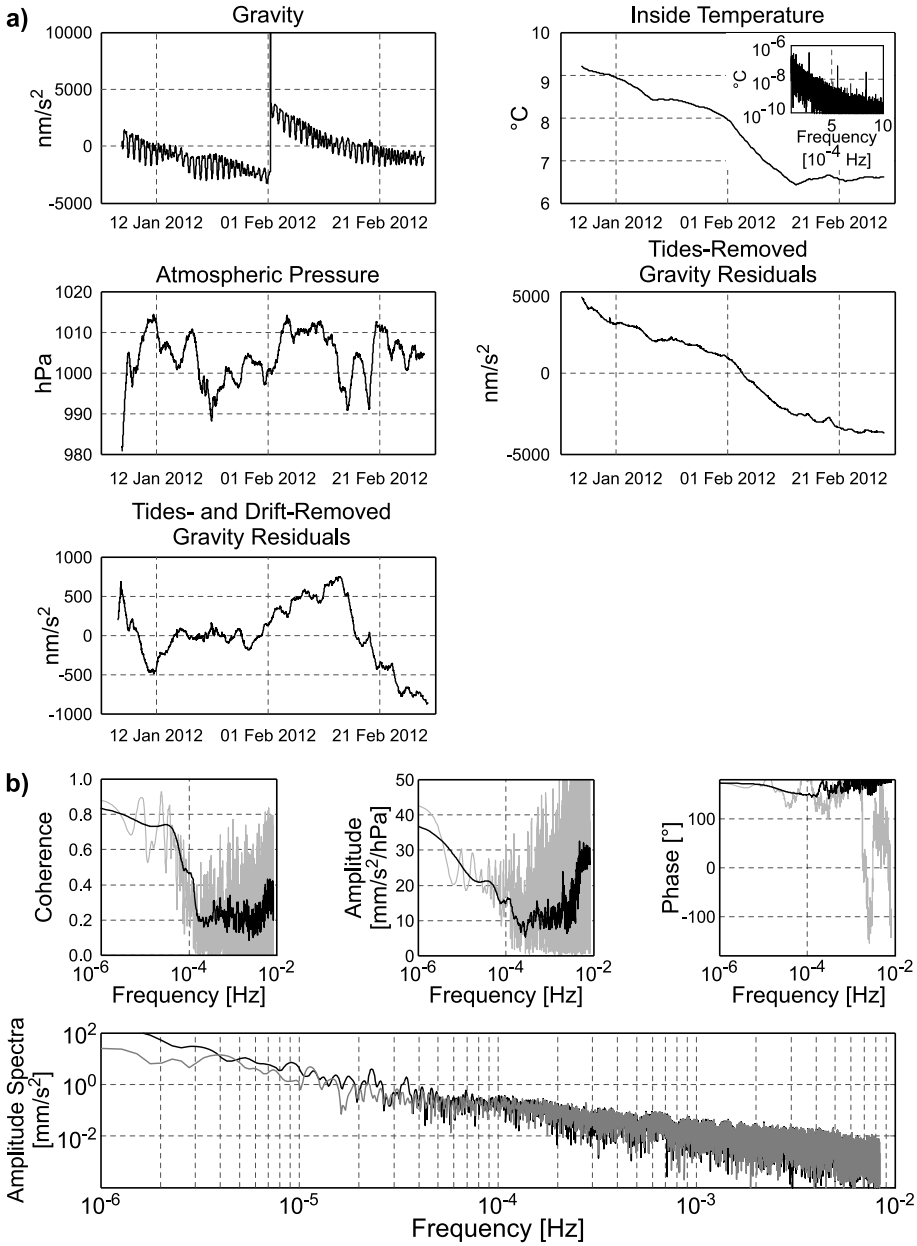

Fig. 7. **a)** Gravity records, tides-removed, tides- and drift-removed gravity residuals, temperature and atmospheric pressure variations of L&R ET-11. **b)** Coherence, amplitude and phase response of L&R ET-11 to pressure changes (smoothing in black), and amplitude spectra of tidal residuals before (in black) and after (in gray) atmospheric pressure reduction using the barometric transfer function.

see an additional signal associated with the buoyancy force on the mass which in ET-gravimeters is partially compensated by the buoyancy compensator on the beam. The apparent admittance is then much larger than the usual values. Since we do not know the pressure inside the sensor, there could be some non-linearity depending on the leakage of the seal. The use of the Hilbert-transform of pressure changes is a zeroth order test to try to remove further this effect using a regression factor, but as the coherence with it is even weaker, we cannot model the pressure effect of this leaky ET-11 gravimeter with such simple barometric models. The frequency admittance and the phase response to atmospheric pressure variations for the L&R ET-11 are plotted in Fig. 7b. We can see that the admittance is about –20 (nm/s^2)/hPa at tidal frequencies and around –10 (nm/s^2)/hPa between 10^{-4} and 10^{-3} Hz (the admittances would be much larger in magnitude if the buoyancy compensator would not be built into the instrument). The atmospheric pressure reduction is slightly efficient only for frequencies below 4×10^{-5} Hz (periods larger than 7 h), i.e. when the coherence becomes larger than 0.5 (cf. lower plot of Fig. 7b). We have also plotted a smoothed version of the coherence and transfer functions by applying a Savitzky-Golay FIR smoothing filter (*Savitzky and Golay, 1964*) which has the advantage not to artificially decrease the coherence and admittance at low-frequencies contrary to the convolution with a Hanning window. In the phase plots (Figs 7b to Fig. 12), the phase was unwrapped with respect to 180°.

The difference in the response of ET005 and ET11 is mostly due to the fact that the effects of air pressure changes on the sensor were negligible in the case of ET005 due to the special sealed container and because of their age the seals of ET-11 are leaky.

For the gPhone-054, the Graviton and the CG5, the low-frequency coherence is very sensitive to the drift correction. For these three gravimeters, we have removed a degree-3 polynomial drift. If a linear drift was removed, the coherence at very low frequencies was unexpectedly weaker. Indeed, for the Graviton and gPhone-054, the drift was clearly not linear during the 15 days considered.

For the gPhone-054, the coherence with atmospheric pressure changes is weaker than for the L&R ET-005 but similar to that with the L&R ET-11 (Fig. 8). In Fig. 8 we have also plotted the frequency-dependent admittance and phase computed over 15 days as well as the tidal residuals before and after atmospheric pressure reduction. In agreement with *Riccardi et al. (2011)*, the barometric admittance is varying between –2 and –4 (nm/s^2)/hPa at tidal frequencies (below 10^{-4} Hz).

The response of the Graviton to atmospheric pressure changes has a non-linear phase behavior at periods longer than 1 h (Fig. 9). The coherence is weaker than for the gPhone but the atmospheric pressure deconvolution succeeded in reducing the spectral noise below 0.1 mHz. Removing a linear drift would lead to admittance values between 10 and 20 (nm/s^2)/hPa instead of the 2 to 10 (nm/s^2)/hPa range values obtained in Fig. 9.

For the CG5, the admittance values are similar to that of the gPhone-054 (Fig. 10) but the phase at tidal frequencies is much more stable around 180° like for the SG.

For the broadband seismometer STS-2, the coherence with atmospheric pressure changes is also very weak (cf. Fig. 11). The admittance is even positive and large at tidal frequencies (around 25 (nm/s^2)/hPa) but reaches a normal behavior in the long-period seismic band (frequencies above 10^{-4} Hz), with a typical V-shape (*Zürn and Wielandt, 2007*; *Zürn and Meurers, 2009*) and a minimum near 3 mHz. The lack of coherency

demonstrates that sources of noise other than the local barometric pressure prevail. Indeed, the STS-2 records are contaminated by the hourly (and its harmonics) temperature variations due to an air conditioning system inside the J9 bunker (cf. the spectral peak in Fig. 11 and the amplitude spectrum of the inside temperature in the insert in Fig. 7a). The L&R ET-11 is located in the same room as the STS-2 but is less sensitive to this hourly air conditioning system because of the buoyancy compensator and the better thermal insulation. Indeed, the associated 1-h spectral peak is much smaller in the L&R ET-11 amplitude spectrum than in the STS-2 spectrum.

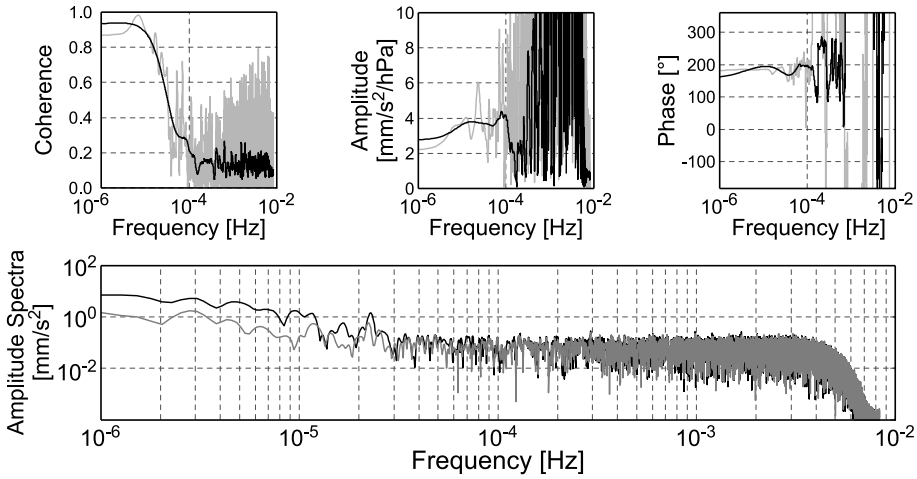

Fig. 8. gPhone-054 response to atmospheric pressure changes: coherence, amplitude and phase response to pressure changes (smoothing in black), and amplitude spectra of tidal residuals before (in black) and after (in gray) atmospheric pressure reduction using the barometric transfer function.

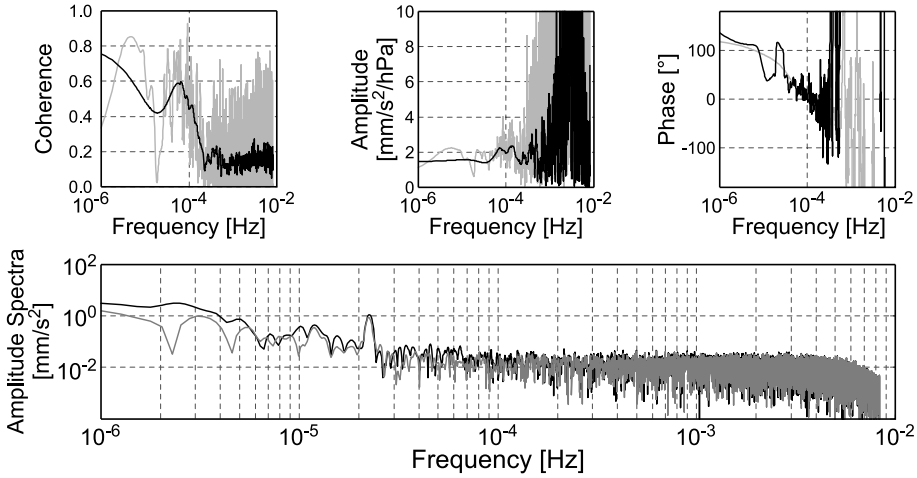

Fig. 9. The same as in Fig. 8, but for the Graviton response.

Finally, we have plotted the transfer function of the SG C026 with atmospheric pressure variations (Fig. 12) to illustrate the well-known shape of the SG response to barometric changes with values around –3.5 (nm/s^2)/hPa at hourly periods (*Merriam, 1992*), then an absolute value decreasing with frequency to reach a minimum around 3.5 mHz. Then the admittance value increases again till the Nyquist frequency (2 min). We refer to the work by *Hinderer et al. (2014)* for a complete study of the SG barometric response at J9 and at a typical equatorial SG site. The latter study stopped the analysis at 3.5 mHz, where the admittance changes its sign (*Zürn and Meurers, 2009*). Indeed, if we enlarge the phase in Fig. 12 we would see that it is around zero between 2 and 4 mHz while it is 180° at other frequencies.

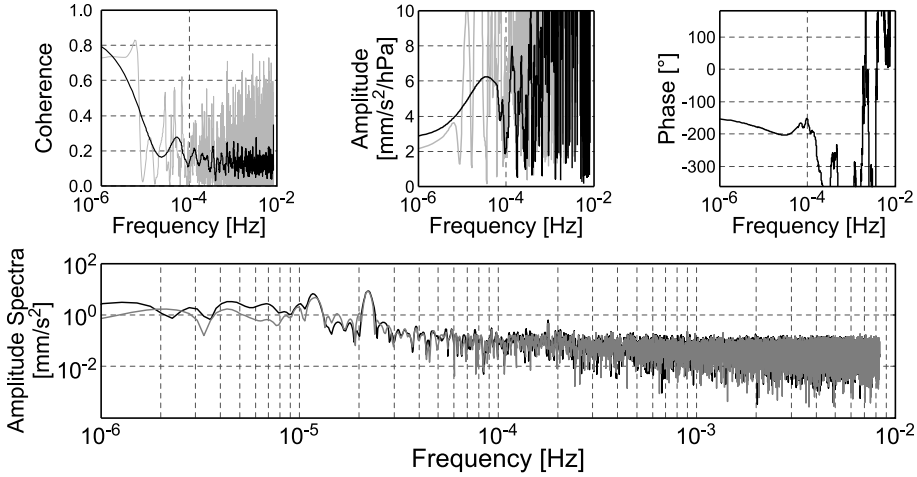

Fig. 10. The same as in Fig. 8, but for the Scintrex CG5 response.

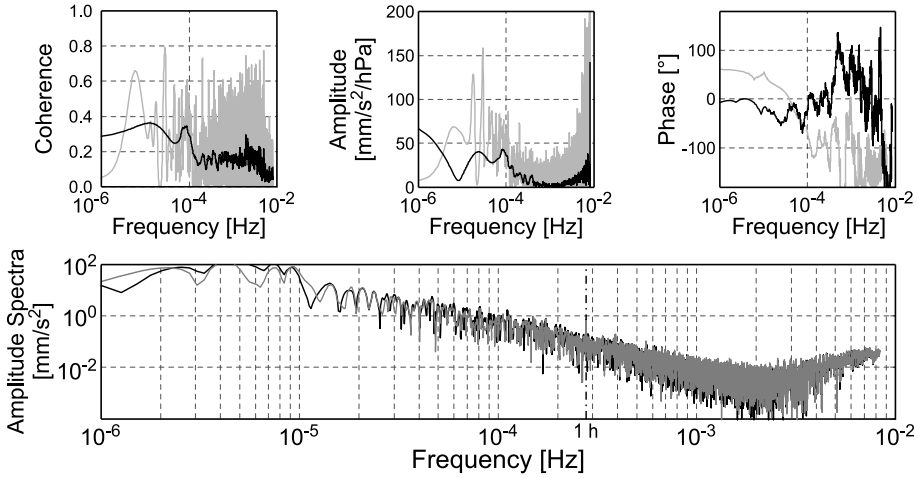

Fig. 11. The same as in Fig. 8, but for the STS-2 response.

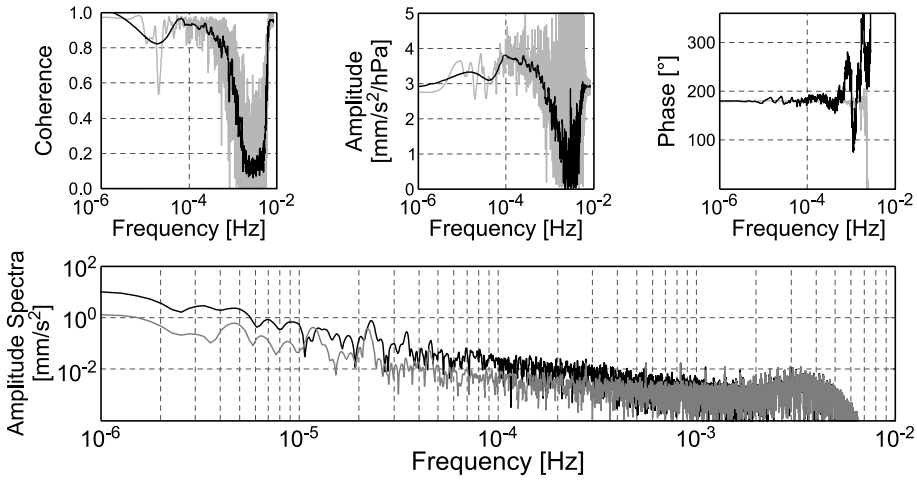

Fig. 12. The same as in Fig. 8, but for the SG C026 response.

For all the gravimeters shown here, we can see a drop of coherence around 2×10^{-5} Hz which corresponds to the semi-diurnal S_2 thermal wave present in the atmospheric pressure records and that has less effect on the gravimeters (*Crossley et al., 1995*).

After having compared the performances of various gravimeters located at J9 Observatory we focus now on simultaneous 1 Hz records from the SG C026, STS-2 and L&R ET-11, in order to retrieve further information on the instrumental self-noise.

4. THREE-CHANNEL CORRELATION ANALYSIS

The noise levels that we have previously estimated for each instrument are the superposition of the Earth's background noise and the instrumental noise. *Sleeman et al. (2006)* have proposed a three-channel correlation analysis to extract the instrument self-noise from the ambient noise. The advantage of using three channels over a two-channel analysis is that we do not need to know the transfer functions. Making the assumptions that the internal noise between two channels is uncorrelated and is uncorrelated to the common input signal, the self-noise power spectral density of channel *i* is given by:

$$N_{ii} = P_{ii} - \frac{P_{ji} P_{ik}}{P_{jk}},$$

where P_{ji} (respectively P_{ik}, P_{jk}) is the cross-*PSD* between channels *j* and *i* (*i* and *k*, *j* and *k*), and P_{ii} is the *PSD* of the recording of channel *i*. The equation for self-noise *PSD* can also be expressed as:

$$N_{ii} = P_{ii} \left(1 - \frac{C_{ji} C_{ik}}{C_{jk}} \right),$$

where C_{ji} (respectively C_{ik}, C_{jk}) is the coherency between channels j and i (i and k, j and k). The noise cross-power spectra N_{ij} (respectively N_{ik}, N_{jk}) of internal noise for channels i and j (i and k, j and k) are assumed to be zero for $i \neq j$ ($i \neq k$, $j \neq k$).

The L&R ET-11 and the STS-2 are both digitized at 1 Hz by a Quanterra Q4120 data logger while the SG C026 data are recorded at 1 Hz by the GWR digital data acquisition unit (DAU). The instrumental noise is the sum of sensor and data acquisition noise. For the study of small geophysical effects, like the incessant background free oscillations, "the so-called "Earth's hum" (e.g. *Nawa et al., 1998*; *Tanimoto, 2008*) or for the ambient noise tomography (e.g. *Shapiro et al., 2005*), the noise of the digital acquisition system (DAU + sensor) should be below the Earth's background noise (environmental noise).

As the three instruments considered here have different band-pass frequencies, the noise characteristics will be different. We will therefore not be able to extract the Quanterra noise or GWR DAU noise independently from the purely sensor noise. However, the cross-correlation may still bring some useful information on the instrument self-noise.

We have performed the cross-correlation analysis on one day of records sampled at 1 Hz. Contrary to *Sleeman et al. (2006)*, we cannot directly use the raw data as the gravimeters are recording gravity acceleration while the STS-2 is recording ground velocity, so the input signal is not the same. So the STS-2 velocity raw output was converted into acceleration by deconvolution in the spectral domain using the nominal poles and zeroes and the Seismic Analysis Code tools (*Helffrich et al., 2013*). For both STS-2 and L&R ET-11 the Quanterra calibration constants were known by some previous calibration experiments and corrected. Contrary to the *PSD* noise levels plotted in previous figures, only a local tidal model (annual, semi-annual, monthly, fortnightly, ter-monthly terms and the principal 10 diurnal, 6 semi-diurnal tides and a higher-frequency component) has been removed and not the atmospheric pressure effects, since the instruments have different responses to atmospheric pressure changes as we have seen in the previous section.

The resulting *PSD*s, self-noise *PSD*s and coherence are plotted in Fig. 13. The *PSD*s have been smoothed using the convolution with a Hanning window. We have also represented the Low-Noise Model of *Peterson (1993)* and the STS-2 noise model of *Wielandt and Widmer-Schnidrig (2002)* for reference. As the SG C026 electronics is equipped with an electronic GGP-1 anti-aliasing low-pass filter which attenuates frequencies larger than 60 mHz, we have also plotted the overall and self-noise *PSD*s with and without deconvolution of the GGP-1 filter. The GGP-1 analog filter response was deconvolved in the frequency domain using the theoretical function of an eight-pole Bessel filter with a corner frequency at 61.5 mHz, a constant time delay of 8.2 s and a 100 dB attenuation at the 0.5 Hz Nyquist frequency (*http://www.gwrinstruments.com/*). Note that the SG instrument response function is flat from very low frequencies to 2 mHz (*Van Camp et al., 2000*) while the velocity response of the STS-2 is roughly flat between 8.33 mHz (120 s) and 10 Hz.

The self-noise *PSD*s (Fig. 13b) show that the SG has higher noise than the ET-11 and STS-2 for frequencies larger than 8 mHz (after deconvolution of the GGP-1 filter). The larger noise amplitude of SG in the free mode band was partly indebted to the Brownian motion of the levitated sphere (*Richter et al., 1995*; *Van Camp, 1999*). Indeed these

authors found a Brownian noise for the SG five times larger than the 10^{-19} m^2s^{-3} limit below which noise can be neglected with respect to seismic noise (*Wielandt and Streckeisen, 1982*). However *Imanishi (2005)* showed that the parasitic mode of the levitated sphere may not be responsible for the enhanced noise level of the SG in the seismic normal mode band.

At periods below 1 mHz, the superiority of gravimeters over STS-2 is also clearly shown by the *PSD*s in Fig. 13. The spikes (already mentioned in Section 2) in the SG self-

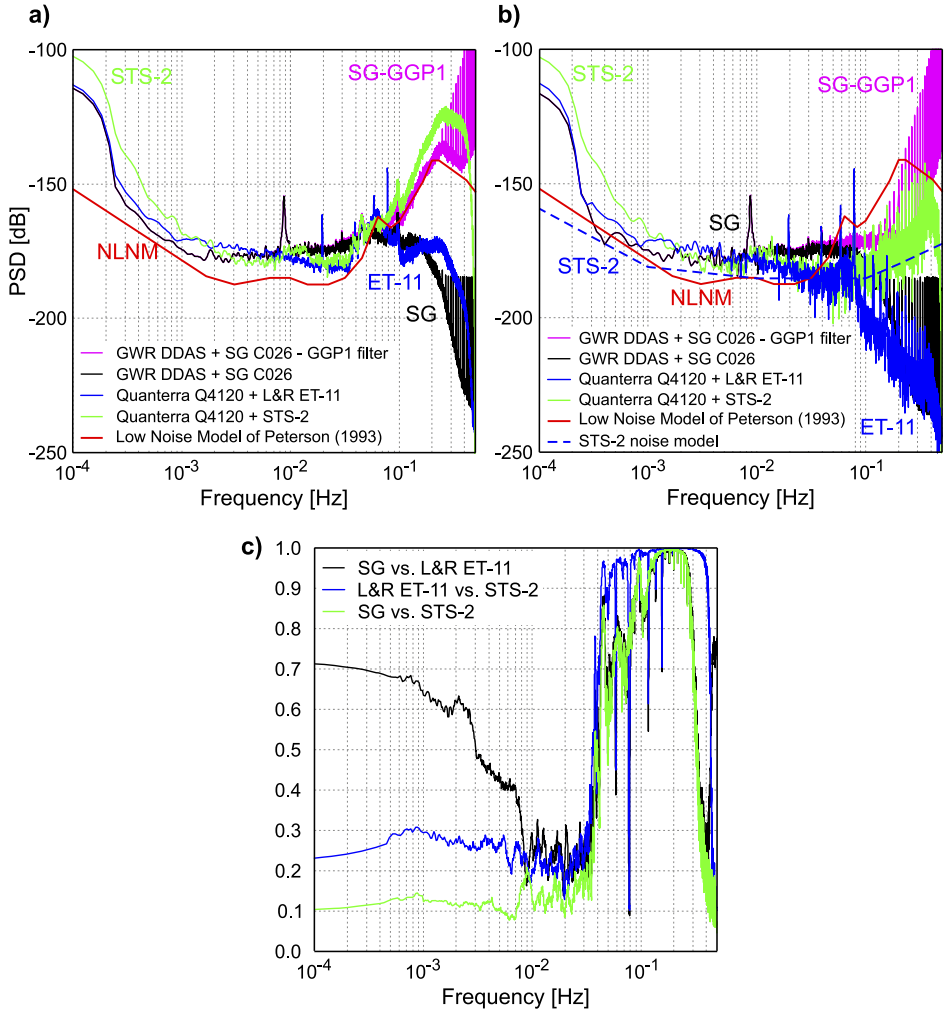

Fig. 13. Three-channel correlation analysis of the 1 Hz SG C026, L&R ET-11 and STS-2 data on one day (31 July 2012). **a)** Power Spectral Densities (*PSD*s) relative to 1 $(m/s^2)^2$/Hz of the data; **b)** *PSD*s relative to 1 $(m/s^2)^2$/Hz of the extracted self-noise (STS-2 self-noise model of *Wielandt and Widmer-Schnidrig (2002)* is shown), and, **c)** coherence.

noise and *PSD* above 0.1 Hz contaminate also the self-noise *PSD*s of the STS-2 and ET-11 through the cross-*PSD*s used in the three-channel correlation procedure. At high frequencies (above 0.1 Hz), the self-noise of the L&R ET-11 is attenuated by its electronics. Contrary to the analog GGP-1 filter, we do not know the characteristics of this low-pass filter.

The resulting self-noise *PSD*s (Fig. 13) have slightly lower values than the overall *PSD*s (Fig. 4) as expected since the ambient noise should have been removed by the procedure. However, we can see that the STS-2 self-noise is above the reference model of *Wielandt and Widmer-Schnidrig (2002)* for frequencies less than 3×10^{-2} Hz, confirming the poor performances of our STS-2 as currently installed in J9.

At long periods (below 2 mHz), the coherence between the SG C026 and L&R ET-11 is much larger than between the L&R ET-11 (or SG C026) and STS-2. This shows the imperfect response of the STS-2 to tides with respect to the gravimeter at such long periods maybe because of some imprecision when deconvolving from the transfer function. A singularity at 0.08 Hz (12.5 s) in the coherence between L&R ET-11 and either SG or STS-2 corresponds to the spectral peak due to the thermostats observed in the *PSD* of the L&R ET-11 (Figs 3 and 4a) and already mentioned above.

The three coherences are minimal between 10 and 20 mHz.

At frequencies larger than 30 mHz, the coherence increases and becomes close to one, particularly between the STS-2 and L&R ET-11 which are both recorded on the Quanterra.

As previously mentioned in Section 2, the noise level of the L&R ET-11 between 10 and 30 mHz is strongly influenced by the behavior of the electronic heater system. When the heater system has a periodic function, the thermal noise concentrates in a very sharp spectral noise (as seen in Fig. 13). However, recently (since 2013), it seems that this function becomes irregular introducing a thermal noise with a broad spectrum. Then we have also plotted in Fig. 14 the overall *PSD*s, self-noise *PSD*s and coherences for June 26, 2013 when the outer heater does not show a periodic behavior. This day is one of the quietest days during the year 2013 for the ET-11 gravimeter. The self-noise *PSD*s (Fig. 14b) show that the SG has higher noise than the ET-11 and STS-2 for frequencies larger than 20 mHz (after deconvolution of the GGP-1 filter). The coherence (Fig. 14c) between the ET-11 and SG or ET-11 and STS-2 is smaller than in Fig. 13c and is around 20% between 8 and 20 mHz. In Fig. 14c the coherence between 8 and 30 mHz of STS-2 with ET-11 is equal to the coherence of SG with STS-2.

In Fig. 14b the self-noise *PSD* of the ET-11 exhibits a bump between 8 and 15 mHz. A similar bump can be observed in the STS-2 self-noise *PSD* (Fig. 13b) and in the mean *PSD* over 5 quiet days (Fig. 4a). It is present in the STS-2 data all over the years 2012 and 2013 as shown for instance by the percentiles of the daily *PSD*s computed over the year 2012 (Fig. 15). For the ET-11, this bump appears only on some few quiet days. It is well-known that the bump in the NLNM background noise between 7 and 30 mHz is due to globe-circling Rayleigh waves (*Ekström, 2001*; *Nishida et al., 2002*; *Widmer-Schnidrig, 2003*). Our observed bump in the STS-2 *PSD*s is probably due to such waves while the one in the ET-11 data may be hidden by the outer heater as it is not persistent.

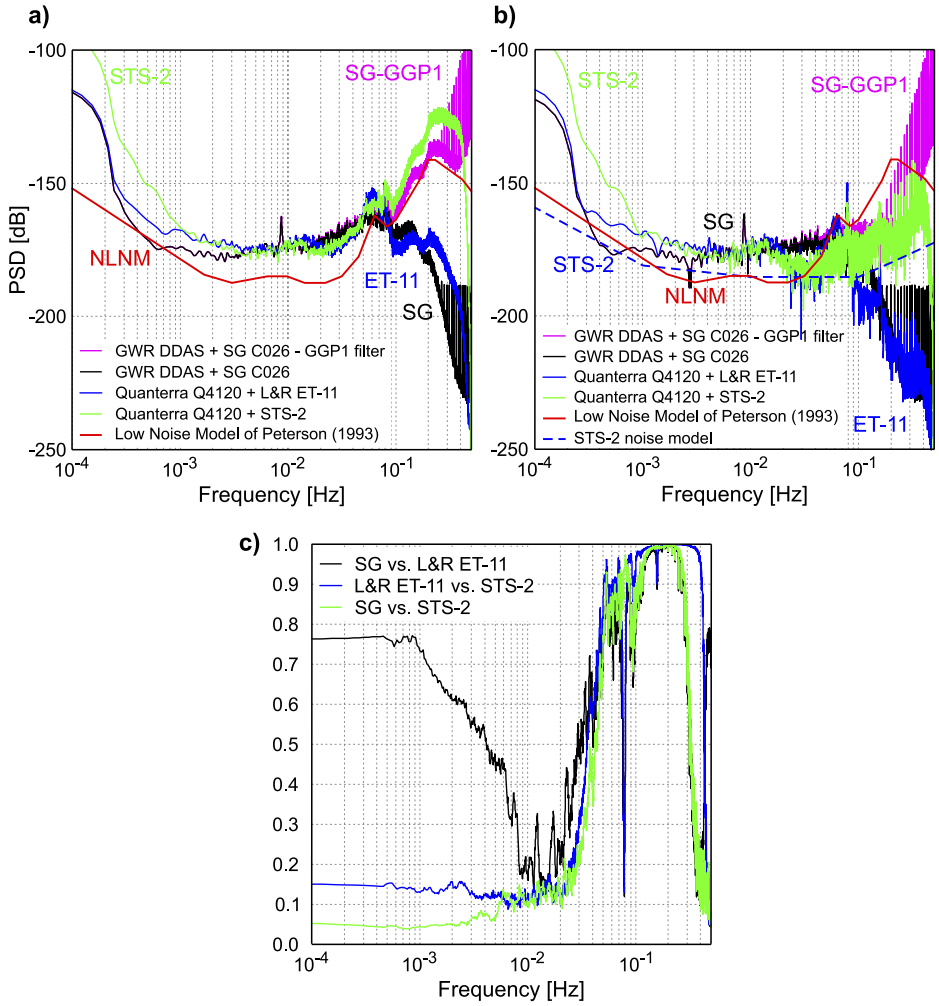

Fig. 14. The same as in Fig. 13, but for 26 June 2013.

5. CONCLUSION

At seismic frequencies, SGs present the lowest noise magnitudes and the other spring gravimeters (gPhone-054, CG5 and Graviton-EG1194) have the highest noise levels, while the ET-gravimeters lie in between. At sub-seismic frequencies, the SGs still have the best performances while the ET-gravimeters and the other spring gravimeters reach similar noise magnitudes. The currently operating L&R ET-11 is not air-tight anymore and hence is noisier than the previous L&R ET-005 (1976–1985) at sub-seismic frequencies. In the long-period seismic band (between 3 and 100 mHz), where the Earth's

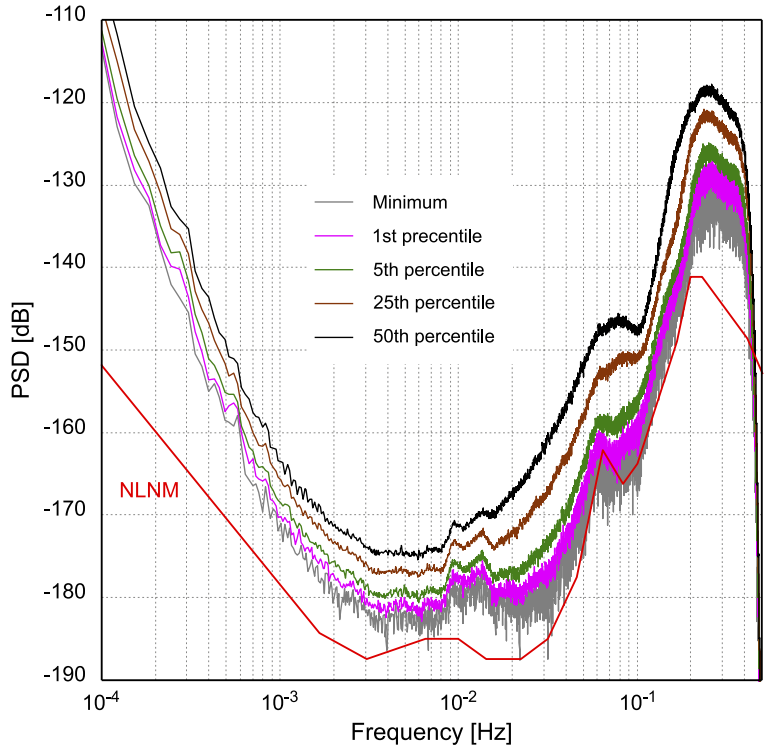

Fig. 15. Statistics on the daily Power Spectral Densities (*PSD*s) relative to 1 $(m/s^2)^2$/Hz of the STS-2 data during the year 2012 showing the minimum, 1st, 5th, 25th and 50th percentiles with respect to the Low Noise Model (NLNM) of *Peterson (1993)*.

background noise is minimal, the SG C026 has a higher self-noise , while the STS-2 and the L&R ET-11 reach their best performances with a flat noise level till about 30 mHz, where the microseismic noise starts. Below 2 mHz the L&R ET-11 and the STS-2 become noisier than the SG-C026. The three-channel correlation analysis has confirmed the better performances of the gravimeters over the long period seismometer STS-2 below 1 mHz and the higher noise level of the SG at frequencies larger than 10 mHz. The origin of this SG instrumental noise is presently unknown.

Acknowledgements: We would like to thank Paul Rydelek who gave the LaCoste & Romberg ET-11 to the Black Forest Observatory before it was installed at J9 by Walter Zürn. We thank also Jean-Yves Thore for his help in connecting the LR-ET11 to the Quanterra Q4120 data-logger and for the extraction of data from the Quanterra. J.A. was supported by project CGL2011-25494 of the Spanish Ministry of Economy and Competitiveness. Constructive comments from Bruno Meurers and an anonymous reviewer are gratefully acknowledged.

References

Abours S. 1977. *Exploitation des enregistrements de marée gravimétrique à Strasbourg - Aout 1973-Février 1977*. Diplôme d'Ingénieur Géophysicien. University of Strasbourg, France (in French).

Abours S. and Lecolazet R., 1977. New results about the dynamical effects of the liquid outer core as observed at Strasbourg. In: Bonatz M. and Melchior P. (Eds), *Proceedings of the 8th International Symposium on Earth Tides: Bonn, 19-24 September 1977*. Institute of Theoretical Geodesy, University of Bonn, Bonn, Germany, 689–697.

Amalvict M., Hinderer J, Boy J.-P. and Gegout P., 2001. A 3 year comparison between a superconducting gravimeter (GWRC026) and an absolute gravimeter (FG5#206) in Strasbourg (France). *J. Geod. Soc. Japan*, **47**, 334–340.

Arnoso J., Vieira R., Velez E.J., Van Ruymbeke M. and Venedikov A.P., 2001. Studies of tides and instrumental performance of three gravimeters at Cueva de los Verdes (Lanzarote, Spain). *J. Geod. Soc. Japan*, **47**, 70–75.

Arnoso J., Riccardi U., Hinderer J., Cordoba B. and Montesinos F.G., 2014. Analysis of co-located measurements made with a LaCoste & Romberg Graviton-EG gravimeter and two superconducting gravimeters at Strasbourg (France) and Yebes (Spain). *Acta Geod. Geophys.*, **49**, 147–160, DOI: 10.1007/s40328-014-0043-y.

Banka D., 1997. *Noise Levels of Superconducting Gravimeters at Seismic Frequencies*. Ph.D. Thesis, University of Clausthal, Clausthal, Germany.

Banka D. and Crossley D., 1999. Noise levels of superconducting gravimeters at seismic frequencies. *Geophys. J. Int.*, **139**, 87–97.

Calvo M., Rosat S., Hinderer J., Legros H., Boy J.-P. and Riccardi U., 2014. Study of the time stability of tides using a long term (1973–2011) gravity record at Strasbourg, France. In: Rizos C. and Willis P. (Eds), *Earth on the Edge: Science for a Sustainable Planet*. International Association of Geodesy Symposia, **139**. Springer-Verlag, Berlin, Germany, 377–381.

Crossley D., Jensen O. and Hinderer J., 1995. Effective barometric admittance and gravity residuals. *Phys. Earth Planet Inter.*, **90**, 221–241.

Crossley D., Hinderer J., Casula G., Francis O., Hsu H.T., Imanishi Y., Jentzsch G., Kääriäinen J., Merriam J., Meurers B., Neumeyer J., Richter B., Shibuya K., Sato T. and Van Dam T., 1999. Network of superconducting gravimeters benefits a number of disciplines. *EOS Trans. AGU*, **80**(11), 121/125–126.

Crossley D., Hinderer J. and Amalvict M., 2001. A spectral comparison of absolute and superconducting gravimeter data. *J. Geod. Soc. Japan*, **47**, 373–379.

Crossley D., Hinderer J. and Riccardi U., 2013. The measurement of surface gravity. *Rep. Prog. Phys.*, **76**, 046101.

Ekström G., 2001. Time domain analysis of the earth's background seismic radiation. *J. Geophys. Res.*, **106**, 26483–26494.

Freybourger M., Hinderer J. and Trampert J., 1997. Comparative study of superconducting gravimeters and broadband seismometers STS-1/Z in subseismic frequency bands. *Phys. Earth Planet. Inter.*, **101**, 203–217.

Gostoli J., 1970. Etude et construction d'un dispositif d'asservissement pour un gravimètre LaCoste-Romberg. Enregistrement numérique de la marée gravimétrique. Thèse de Dr. Ing., University of Strasbourg, Strasbourg, France (in French).

Helffrich G.R., Wookey J.M. and Bastow I.D., 2013. *The Seismic Analysis Code: A Primer and User's Guide*. Cambridge University Press, Cambridge, U.K.

Hinderer J., Amalvict M., Crossley D., Leveque J.-J., Rivera L. and Luck B., 2002. Tides, earthquakes and ground noise as seen by the absolute gravimeter FG5 and its superspring; comparison with a superconducting gravimeter and a broadband seismometer. *Metrologia*, **39**, 495–501.

Hinderer J., Hector B., Boy J.-P., Riccardi U., Rosat S., Calvo M. and Littel F, 2014. A search for atmospheric effects on gravity at different time and space scales. *J. Geodyn.*, **80**, 50–57, DOI: 10.1016/j.jog.2014.02.001.

Imanishi Y., 2005. On the possible cause of long period instrumental noise (parasitic mode) of a superconducting gravimeter. *J. Geodesy*, **78**, 683–690.

Imanishi Y., 2009. High-frequency parasitic modes of superconducting gravimeters. *J. Geodesy*, **83**, 455–467.

Kurrle D. and Widmer-Schnidrig R., 2008. The horizontal hum of the Earth: A global background of spheroidal and toroidal modes. *Geophys. Res. Lett*., **35**, DOI: 10.1029/2007GL033125.

LaCoste & Romberg, 2004. *Instruction Manual Model G and D Meters*. LaCoste & Romberg, Austin, TX, 127 pp.

Merriam J., 1992. Atmospheric pressure and gravity. *Geophys. J. Int*., **109**, 488–500.

Meurers B., 2002. Aspects of gravimeter calibration by time domain comparison of gravity records. *Bull. Inf. Marées Terr.*, **135**, 10643–10650.

Nawa K., Suda N., Fukao Y., Sato T., Aoyama Y. and Shibuya K., 1998. Incessant excitation of the Earth's free oscillations. *Earth Planets Space*, **136**, 3–8.

Niebauer T., 2007. Gravimetric methods - absolute gravimeter: instruments concepts and implementation. In: Herring T. (Ed.), *Treatise on Geophysics, Volume 3 - Geodesy.* Elsevier, Amsterdam, The Netherlands, 43–64.

Nishida K., Kobayashi N. and Fukao Y., 2002. Origin of Earth's ground noise from 2 to 20 mHz. *Geophys. Res. Lett*., **29**, 52-1–52-4.

Peterson J., 1993. *Observations and Modelling of Seismic Background Noise*. Open-File Report 93-332. U.S. Department of Interior, Geological Survey, Albuquerque, NM.

Riccardi U., Rosat S. and Hinderer J., 2011. Comparison of the Micro-g LaCoste gPhone-054 spring gravimeter and the GWR-C026 superconducting gravimeter in Strasbourg (France) using a 300-day time series. *Metrologia*, **48**, 28–39.

Richter B., Wenzel H.-G., Zürn W. and Klopping F., 1995. From chandler wobble to free oscillations: comparison of cryogenic gravimeters and other instruments in a wide period range. *Phys. Earth Planet. Inter.*, **91**, 131–148.

Rosat S., Boy J.-P., Ferhat G., Hinderer J., Amalvict M., Gegout P. and Luck B., 2009. Analysis of a ten-year (1997–2007) record of time varying gravity in Strasbourg using absolute and superconducting gravimeters: new results on the calibration and comparison with GPS height changes and hydrology. *J. Geodyn*., **48**, 360–365.

Rosat S. and Hinderer J., 2011. Noise levels of superconducting gravimeters: updated comparison and time stability. *Bull. Seismol. Soc. Amer.*, **101**, 1233–1241.

Rosat S., Hinderer J., Crossley D. and Boy J.P., 2004. Performance of superconducting gravimeters from long-period seismology to tides. *J. Geodyn*., **38**, 461–476.

Savitzky A. and Golay M.J.E., 1964. Smoothing and differentiation of data by simplified least squares procedures. *Anal. Chem.*, **36**, 1627–1639.

Shapiro N.M, Campillo M., Stehly L. and Ritzwoller M.H., 2005. High-resolution surface-wave tomography from ambient seismic noise. *Science*, **307**, 1615–1618.

Sleeman R., van Wettum A. and Trampert J., 2006. Three-channel correlation analysis: a new technique to measure instrumental noise of digitizers and seismic sensors. *Bull. Seismol. Soc. Amer.*, **96**, 258–271.

Tanimoto T., 2008. *Humming a different tune*. *Nature*, **452**, 539–541.

Van Camp M., 1999. Measuring seismic normal modes with the GWR C021 superconducting gravimeter. *Phys. Earth Planet. Inter.*, **116**, 81–92.

Van Camp M., Wenzel H.-G., Schott P., Vauterin P. and Francis O., 2000. Accurate transfer function determination for superconducting gravimeters. *Geophys. Res. Lett*., **27**, 37–40.

Van Camp M., Williams S.D.P. and Francis O., 2005. Uncertainty of absolute gravity measurements. *J. Geophys. Res.*, **110**, B05406, DOI: 10.1029/2004JB003497.

Webb S.C., 2007. The Earth's "hum" is driven by ocean waves over the continental shelves. *Nature*, **445**, 754–756, DOI: 10.1038/nature05536.

Widmer R. and Zürn W., 1995. On noise reduction in vertical seismic records below 2 mHz using local barometric pressure. *Geophys. Res. Lett*., **22**, 3537–3540.

Widmer-Schnidrig R., 2003. What can superconducting gravimeters contribute to normal-mode seismology? *Bull. Seismol. Soc. Amer.*, **93**, 1370–1380.

Wielandt E. and Streckeisen G., 1982. The leaf spring seismometer: design and performance. *Bull. Seismol. Soc. Amer.*, **72**, 2349–2367.

Wielandt E. and Widmer-Schnidrig R., 2002. Seismic sensing and seismic noise. In: Korn M. (Ed.), *Ten Years of German Regional Seismic Network (GRSN)*. Report 25. Senate Commission for Geosciences. Wiley-VCH Verlag GmbH, Weinheim, Germany.

Zürn W., Wenzel H.-G. and Laske G., 1991. High quality data from LaCoste-Romberg gravimeters with electrostatic feedback: A challenge for superconducting gravimeters. *Bull. Inf. Marées Terr*., **110**, 79440–7952.

Zürn W., Exss J., Steffen H., Kroner C., Jahr T. and Westerhaus M., 2007. On reduction of long-period horizontal seismic noise using local barometric pressure. *Geophys. J. Int.*, **171**, 780–796.

Zürn W. and Meurers B., 2009. Clear evidence for the sign-reversal of the pressure admittance to gravity near 3mHz. *J. Geodyn.*, **48**, 371–377.

Zürn W. and Wielandt E., 2007. On the minimum of vertical seismic noise near 3 mHz. *Geophys. J. Int.*, **168**, 647–658.